Ocean Dynamics (2017) 67:1481–1494
DOI 10.1007/s10236-017-1092-x

Modeling spring-summer phytoplankton bloom in Lake Michigan with and without riverine nutrient loading

Lin Luo[1] · Jia Wang[2] · Timothy Hunter[2] · Dongxiao Wang[1] · Henry A. Vanderploeg[2]

Received: 14 October 2016 / Accepted: 10 August 2017 / Published online: 7 September 2017
© US Government (outside the USA) 2017

Abstract There were two phytoplankton blooms captured by remote sensing in Lake Michigan in 1998, one from March to May, and one during June. In this paper, those phytoplankton blooms were simulated by a coupled physical–biological model, driven by observed meteorological forcing in 1998. The model reasonably reproduced the lake currents. The biological model results, with and without riverine nutrient loading, were compared with the remote sensing data. A 3-month-long donut-like phytoplankton bloom that appeared in southern Lake Michigan was reasonably well simulated only when riverine input was included, indicating the importance of riverine nutrient input for supporting the growth of phytoplankton in Lake Michigan. The model with riverine input also captured a second event-driven phytoplankton bloom during June with weaker magnitude that occurred in mid-south Lake Michigan, which lasted for about 20 days. The major reason for the weaker bloom in June was that vertical mixing in the hydrodynamic model was too weak (leading to a mixed-layer depth of 20 m) to bring the bottom nutrient-rich water up to the epilimnion. High chlorophyll concentration that persisted in Green Bay for almost a year was simulated with less intensity.

Keywords Phytoplankton bloom · Coupled physical-biological model · Lake Michigan · Great Lakes

This article is part of the Topical Collection on the *8th International Workshop on Modeling the Ocean (IWMO), Bologna, Italy, 7–10 June 2016*

Responsible Editor: Tal Ezer

✉ Jia Wang
jia.wang@noaa.gov

[1] State Key Laboratory of Tropical Oceanography, South China Sea Institute of Oceanology, Chinese Academy of Sciences, Guangzhou, China

[2] NOAA Great Lakes Environmental Research Laboratory, Ann Arbor, MI, USA

1 Introduction

Lake Michigan is a typical phosphorus-limiting aquatic system (Chapra and Sonzogni, 1979). Satellite imagery reveals that high chlorophyll concentrations appear along the coast in spring. This algal bloom in southern Lake Michigan looks like a ring and, thus, is called a chl-a "donut" ring (Lesht et al. 2002; Kerfoot et al. 2008).

There are few modeling studies of the physical–biological processes in the Great Lakes. The episodic bloom event over the time scale of 5–7 days was investigated using a Princeton Ocean Model (POM) coupled with an ecosystem model (Ji et al., 2002; Chen et al., 2004). They simulated and examined the influence of episodic resuspension plume events on the spring bloom in March using a coupled biological and physical model. Stormy weather driving the suspended sediment plumes was emphasized. However, from the satellite images, the bloom ring was observed for 2 months and disappeared in late June 1998.

White et al. (2012) applied a coupled model based on ROMS (Rutgers Ocean Model System) to simulate Lake Superior's physical and ecological processes. They investigated seasonal and interannual variability of lake ice, physical forcing, and the related ecosystem dynamics. Bennington et al. (2012) conducted a modeling study of carbon budget in Lake Superior. The physical model is MITgcm (Bennington et al. 2010), and the ecosystem model includes carbon, phosphorus, oxygen, and alkalinity. River inputs were

included in the study, which motivated this study by adding riverine input to Lake Michigan. Seasonal and year-to-year changes of carbon cycling and related variables were investigated. A similar model was applied to Lake Michigan by Pilcher et al. (2015) with no riverine input. They focused on seasonal cycling of carbon and lower trophic level ecosystem including primary productivity, prior to quagga mussel establishment (2000), i.e., the biological model does not include either quagga or zebra mussel compartment. Oveisy et al. (2014) used ELCOM-CAEDYM (Estuary, Lake and Coastal Ocean Model—Computational Aquatic Ecosystem Dynamics Model) to simulate Lake Erie's hydrodynamics, ice, and simple water quality for the 2004/05 ice season. Rowe et al. (2015) applied a 1-D biological model to investigate the impacts of quagga mussel filtering on phytoplankton and zooplankton dynamics in Lake Michigan.

Luo et al. (2012), for the first time, applied a 3-D coupled physical–biological model, based on FVCOM (finite volume coastal ocean model), to simulate the Lake Michigan spring bloom. The model reproduced a donut-like spring bloom in southern Lake Michigan. However, because the model did not include river-loaded nutrients (Bennington et al. 2012), the simulated spring bloom only lasted less than 2 months (from March to April) and disappeared completely in May, while measurements show the bloom persisted until June. Also, the simulated spring bloom was weaker along the coast than the observed bloom.

From March to May in 1998, there was a circle-like phytoplankton bloom in southern Lake Michigan that was captured in satellite images. The typical formation of the "donut" structure was obvious in March and April and weakened in May. The bloom is regarded to be the result of coupled physical and biological processes. In a previous study, the formation mechanisms of the prolonged spring bloom were investigated by our 3-D coupled physical–biological model, which excluded phosphorus loading from rivers. It was confirmed that this phytoplankton bloom was forced by rapidly increasing temperature and light intensity in spring. The thermal front that develops in spring inhibits the transport of nutrients and phytoplankton from the nearshore to the deeper water. Luo et al. (2012) also showed that the wind-driven gyre circulation in southern Lake Michigan induces significant offshore transport, which contributes to the establishment of the circular bloom. However, only a weak bloom in March was reproduced, which might be caused by lack of external river input of nutrients, since temperature and light intensity were low and contributed little to the phytoplankton growth in March.

The purpose of this paper is to introduce river-loaded nutrients to the existing 3-D NPZD (nutrient-phytoplankton-zooplankton-detritus) model based on FVCOM (Luo et al. 2012) to investigate the mechanisms of the seasonal, prolonged spring–early summer bloom in Lake Michigan. In a previous study, we simulated the spring bloom in Lake Michigan without the riverine nutrient input. The formation mechanisms of the bloom were determined using the coupled physical–biological processes; nevertheless, the bloom was short-lived, only during the spring. In this study, we further investigate the lower trophic level ecosystem dynamics of Lake Michigan with river-loaded nutrients.

2 Methods and data

2.1 Models

The three-dimensional coupled physical–biological model is based on the unstructured grid, FVCOM developed by Chen et al. [2006]. FVCOM is a prognostic, free-surface, 3-D primitive equation coastal ocean circulation model which contains a number of options and components (http://fvcom.smast.umassd.edu/fvcom/), and a flexible biological module (FBM) is included to study food web dynamics. The model was applied to study the hydrodynamics and ecological processes in some estuaries and shelf regions [Li et al. 2014; Tian et al. 2014; Wang et al. 2015], including the Great Lakes [Bai et al. 2013; Luo et al. 2012]. A wind-wave mixing parameterization developed by Hu and Wang [2010] was implemented into the model, which improved the modeled thermal structure and the mixed layer of the water column in the lake [Luo et al. 2012].

The FBM model in this study is simplified to a NPZD model. The four components of the biological model are nutrient (N), phytoplankton (P), zooplankton (Z), and detritus (D). Phosphorus represents the nutrient since it is the limiting element in Lake Michigan. The biological processes among the four components are presented in Fig. 2. The governing equations for the biological variables are given as:

$$\frac{\partial N}{\partial t}+u\frac{\partial N}{\partial x}+v\frac{\partial N}{\partial y}+w\frac{\partial N}{\partial z}-\frac{\partial}{\partial z}\left(A_h\frac{\partial N}{\partial z}\right)-\frac{\partial}{\partial x}\left(A_w\frac{\partial N}{\partial x}\right)-\frac{\partial}{\partial y}\left(A_w\frac{\partial N}{\partial y}\right) = -\mathrm{P(uptake)}+\mathrm{Z(respiration)}+\mathrm{P(respiration)}+\mathrm{D(remineralization)} \quad (1)$$

$$\frac{\partial P}{\partial t}+u\frac{\partial P}{\partial x}+v\frac{\partial P}{\partial y}+w\frac{\partial P}{\partial z}-\frac{\partial}{\partial z}\left(A_h\frac{\partial P}{\partial z}\right)-\frac{\partial}{\partial x}\left(A_w\frac{\partial P}{\partial x}\right)-\frac{\partial}{\partial y}\left(A_w\frac{\partial P}{\partial y}\right) = \mathrm{P(uptake)}-\mathrm{P(respiration)}-\mathrm{P(mortality)}-\mathrm{Z}P\mathrm{(grazing)}-\mathrm{P(sinking)} \quad (2)$$

$$\frac{\partial Z}{\partial t}+u\frac{\partial Z}{\partial x}+v\frac{\partial Z}{\partial y}+w\frac{\partial Z}{\partial z}-\frac{\partial}{\partial z}\left(A_h\frac{\partial Z}{\partial z}\right)-\frac{\partial}{\partial x}\left(A_w\frac{\partial Z}{\partial x}\right)-\frac{\partial}{\partial y}\left(A_w\frac{\partial Z}{\partial y}\right) = \mathrm{ZP(grazing)}+\mathrm{ZD(grazing)}-\mathrm{Z\ (respiration)}-\mathrm{Z\ (mortality)} \quad (3)$$

$$\frac{\partial D}{\partial t}+u\frac{\partial D}{\partial x}+v\frac{\partial D}{\partial y}+w\frac{\partial D}{\partial z}-\frac{\partial}{\partial z}\left(A_h\frac{\partial D}{\partial z}\right)-\frac{\partial}{\partial x}\left(A_w\frac{\partial D}{\partial x}\right)-\frac{\partial}{\partial y}\left(A_w\frac{\partial D}{\partial y}\right) = \mathrm{P(mortality)}+\mathrm{Z(mortality)}+\mathrm{(grazingloss)}-\mathrm{ZD(grazing)}-\mathrm{D(remineraliztion)}-\mathrm{D(sinking)} \quad (4)$$

In the derivative operator, x, y, and z are the eastward, northward, and vertical axes of the Cartesian coordinate and

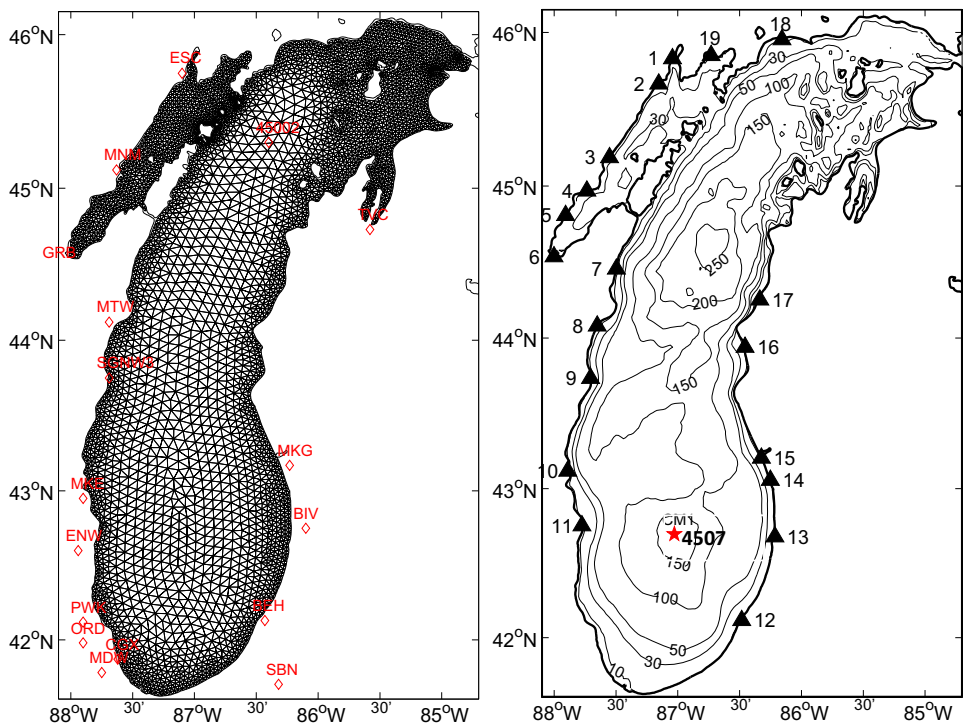

Fig. 1 (*left*) Model grid and weather stations from which atmospheric forcings were derived (see Luo et al. (2012) for detail) and (*right*) model topography of Lake Michigan. The *solid triangles* indicate the 19 main rivers around the lake (Table 1)

u, v, and *w* are the x, y, and z components of the velocity. A_w and A_h are the horizontal and thermal diffusion coefficients. Chlorophyll concentration is derived from the phytoplankton as a ratio of chlorophyll to carbon.

2.2 Model setting

The Lake Michigan high-resolution bathymetric grid is based on the NOAA National Geophysical Data Center (http://www.ngdc.noaa.gov/mgg/greatlakes/greatlakes.html). The model grid consists of 9054 elements and 4981 nodes in the horizontal (Fig. 1) and 21 sigma levels in the vertical. The resolution is higher near the surface and the bottom boundary layer. The minimum depth was set to 5 m according to the stability condition, $h_{min} + \zeta_{max} > 0$, where h_{min} is the minimum water depth and ζ_{max} is the maximum water elevation, due to strong (gust) winds and storm surges along the coast (Wang, 1996). Based on the Courant–Friedrichs–Lewy (CFL) criterion, one of the global stability conditions, the internal mode time step of the numerical integration is 180 s, while the external mode time step is 18 s. The model was spun up over 2 months, starting on January 1, 1998 and ran for 1 year (Fig. 2).

The physical model is driven by observed hourly winds and heat flux calculated from the meteorological observations around Lake Michigan (Fig. 1). The heat flux includes two parts: the surface net heat flux and the penetrated short-wave irradiance, which are also the factors responsible for the growth of phytoplankton.

The biological model is run simultaneously with the physical model. The initial values of phosphorus, phytoplankton, zooplankton, and detritus were given as 0.1 mmol P/m^3, 0.5 mmol C/m^3, 0.7 mmol C/m^3, and 6.5 mmol C/m^3 based on the previous literature values [Chen et al., 2002, 2004]. The initial conditions of biological variables are spatially uniform, since the water column is vertically well mixed in winter. The mathematical expressions for each term of Eqs. (1)–(4) are given in Appendix A, and the parameters used are listed in Appendix B.

In this study, the point source inputs from rivers (Lesht et al. 1991) were taken into account. Nineteen tributaries around Lake Michigan were used (Fig. 1, right; Table 1).

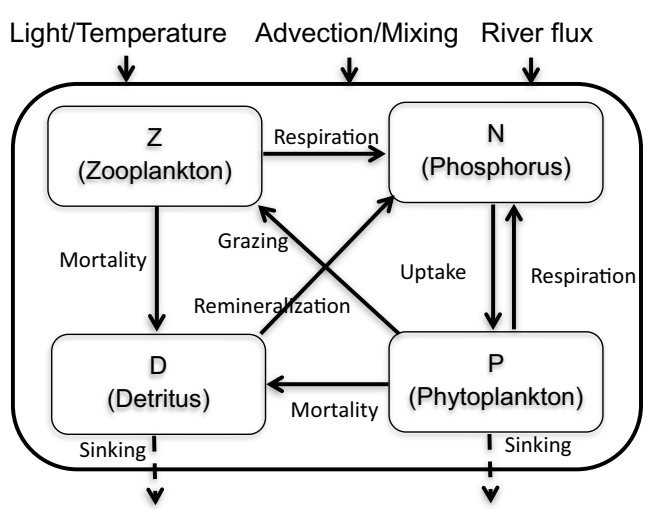

Fig. 2 Schematic of the biological model in Lake Michigan

Table 1 The runoff and nutrient load of 19 rivers and Straits of Mackinac (see Fig. 1, right) are included in this study

No	River	No	River
1	Escanaba	11	Root
2	Ford	12	St. Joseph
3	Menominee	13	Kalamazoo
4	Peshtigo	14	Grand
5	Oconto	15	Muskegon
6	Fox	16	Pere Marquette
7	Kewaunee	17	Manistee
8	Manitowoc	18	Manistique
9	Sheboygan	19	Sturgeon
10	Milwaukee	20	Straits of Mackinac

The seasonal cycle time series of river discharges and loaded phosphorus of the largest four rivers are shown in Fig. 3, and the data originate from the US Geological Survey. The flow from the Straits of Mackinac to Lake Huron is also included based on the previous studies of water transport through the Straits [Saylor and Sloss, 1976; Powers and Ayers, 1960].

2.3 Calibration data

Satellite-retrieved chlorophyll concentration was derived from SeaWiFS (Sea-viewing Wide Field-of-view Sensor, http://oceandata.sci. gsfc.nasa.gov/SeaWiFS). The satellite measurements were used to validate the temporal variations and spatial patterns of the simulated chlorophyll pattern.

Because optical properties are highly influence by colored dissolved organic matter (CDOM), which hinders the retrieval of chlorophyll concentration, Mouw et al. (2013) proposed an algorithm to correct the NASA (OC3) algorithm in Lake Superior. The absorption due to CDOM has spatial variability: greatest in the western arm of Lake Superior and near river mouths and decrease with distance offshore (see their Fig. 11).

Shuchman et al. (2013) applied a similar method, called the Colored Producing Agent (CPA) algorithm, to Lake Michigan. A single average hydro-optical model for the Great Lakes was found to generate insufficiently accurate concentrations for Lakes Michigan, Erie, Superior, and Huron. These new individual lake retrievals were evaluated with respect to EPA in situ field observations, as well as compared to the widely used OC3 MODIS retrieval. The new algorithm retrievals provided slightly more accurate chl values for Lakes Michigan, Superior, Huron, and Ontario than those obtained using the OC3 approach. The CPA algorithm chl retrieval for Lake Erie is quite robust, producing reliable chl values in the reported EPA concentration ranges. However, in Lake Michigan, the CPA algorithm only improves slightly (r^2 = 0.78), compared to the OC3 algorithm (r^2 = 0.74) with limited (19) data points taken only during 2000–2011 (see their Fig. 5).

In situ measurements taken during 1998 (model year) EEGLE (Episodic Events-Great Lakes Experiment: https://www.glerl.noaa.gov/res/projects/eegle/) from regular seven transects (Chicago, Gary, Muskegon, New Buffalo, Racine, Saugatuck, and St. Joseph) and six ship-towed transects were used to calculate the average surface chl-a. The in situ measured chl-a was compared to CPA and NASA data in the model year 1998.

To measure the model's skill for reproducing the measurements, several statistical measures following Wang et al. [2010] were introduced, including mean value, STD (standard deviation, σ), MBD (mean bias deviation), and RMSD (root mean square deviation). They are defined as:

$$\sigma = \sqrt{\frac{1}{n}\sum_{i=1}^{n}\left(x_i - \overline{x}\right)^2}$$

$$\mathrm{MBD} = 100\frac{\frac{1}{n}\sum_{i=1}^{n}(x_i - y_i)}{\frac{1}{n}\sum_{i=1}^{n} y_i} = 100\frac{\overline{X} - \overline{Y}}{\overline{Y}}$$

$$RMSD = \left[\frac{\sum_{i=1}^{n}(x_i - y_i)^2}{n}\right]^{1/2}$$

where x_i and y_i (i = 1, 2, 3, … n) are the modeled and observed time series of any variables such as T, chl-a, etc., n is the total sampling number, and the overbars denote the average of the time series. Standard deviation measures the amount of variation or dispersion from the average. MBD directly measures the relative bias or error of the modeled time series from the observed in percentage. RMSD measures the absolute error of the modeled time series against observation.

3 Results and discussion

3.1 General circulation

Long-term current measurements indicate that annual circulation patterns tend to be cyclonic (counterclockwise) in Lake Michigan with a cyclonic circulation in winter [Beletsky et al., 1999]. A 10-year continuous modeling study of lake hydrodynamics from 1998 to 2007 also showed a remarkably stable large-scale cyclonic circulation pattern during both stratified and unstratified conditions [Beletsky and Schwab, 2001, 2008]. Figure 4 compares the observed and modeled current. The coastal currents along both east and west coasts were strong throughout the year. Lake-averaged mean current speed in Lake Michigan is about 1.9 cm/s based on observation data,

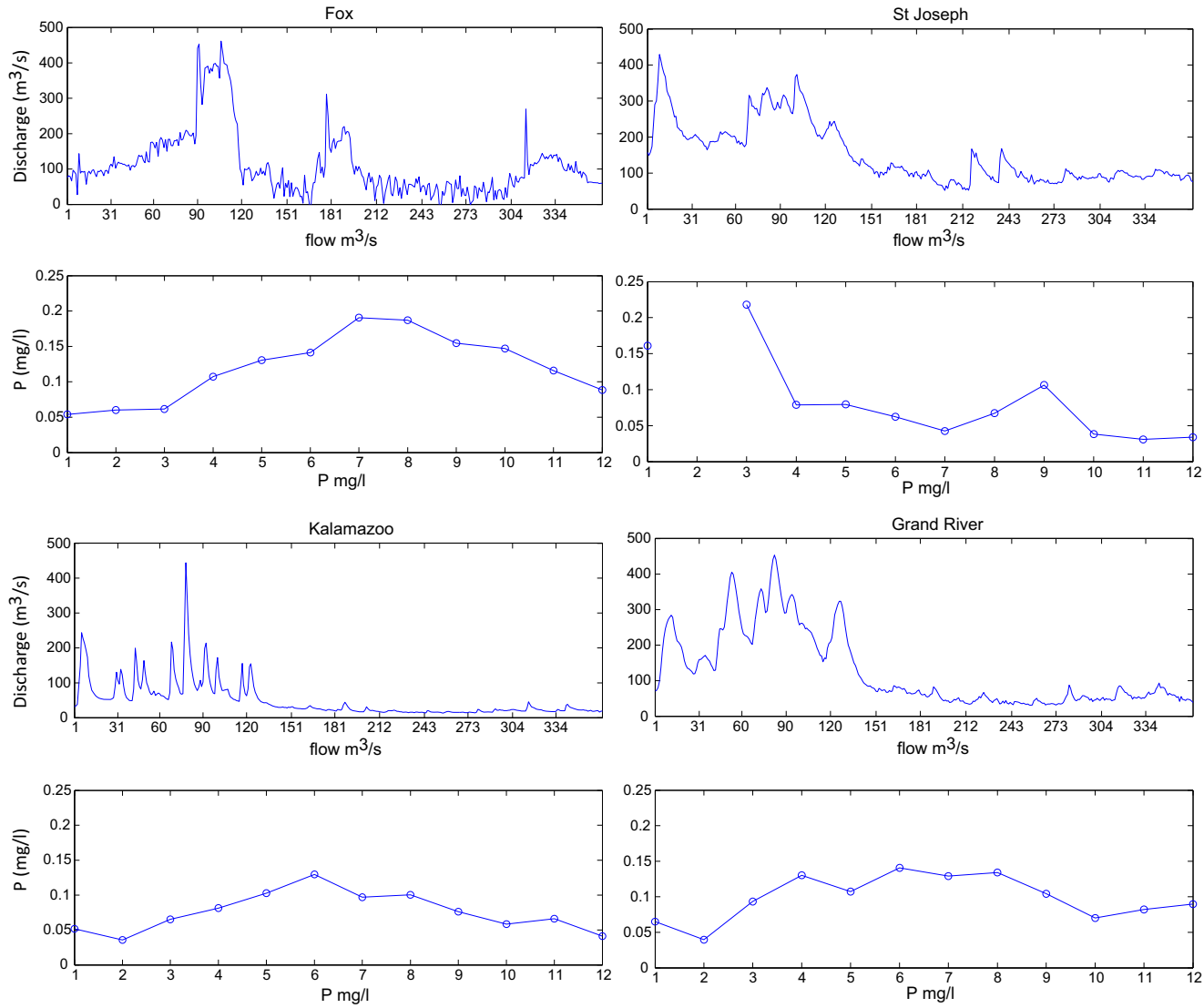

Fig. 3 Seasonal cycle time series of river discharge (in m^3/s) and river-loaded phosphorus (in mg/l) in four large rivers: Fox (6), St. Joseph (12), Kalamazoo (13), and Grand River (14)

and about 1.1 cm/s in our model. The water temperature and thermal structure were validated and discussed in Luo et al. (2012) and will not be presented here. These simulated features are consistent with t he previous model results of Beletsky et al. (2003, 2006).

3.2 Seasonal phytoplankton dynamics

To confirm that the satellite-observed SeaWiFS chl-a data using NASA algorithm are reliable, we examined the observed chl-a data using CPA algorithm by Shuchman et al. (2013). It was found that the chl-a values using CPA algorithm were systematically higher than those using the NASA (OC3) algorithm by nearly double. From October to December, 1998, the values using CPA algorithm were more than twice the NASA data (Fig. 5). For example, the lake-wide average value of chl-a was 4.3 mg/m^3, three times the value of 1.4 mg/m^3 derived from NASA algorithm, which was higher than the spring bloom (3 mg/m^3 in April). Vanderploeg et al. (2007) showed that results of measured surface chl-a (grab samples and transects with calibrated fluorometer) were about 2.2 μg/L during March. During autumn of 1998 in the EEGLE program for the southern basin of Lake Michigan, the chl-a values were consistent with the SeaWiFS algorithm. The CPA algorithm gives results that are too high by a factor of more than two in autumn.

To further validate that the CPA data were higher than the observations, we used in situ measurements along the 1998 EEGLE regular seven transects and six ship-towed transects. The spatial surface chl-a data were averaged, which are also shown in Fig. 5 (in dots). The in situ measured surface chl-a data agree better with SeaWiFS than CPA data in 1998. Mouw et al. (2013) indicated that in Lake Superior, due to CDOM, the SeaWiFS algorithm contains large uncertainly in

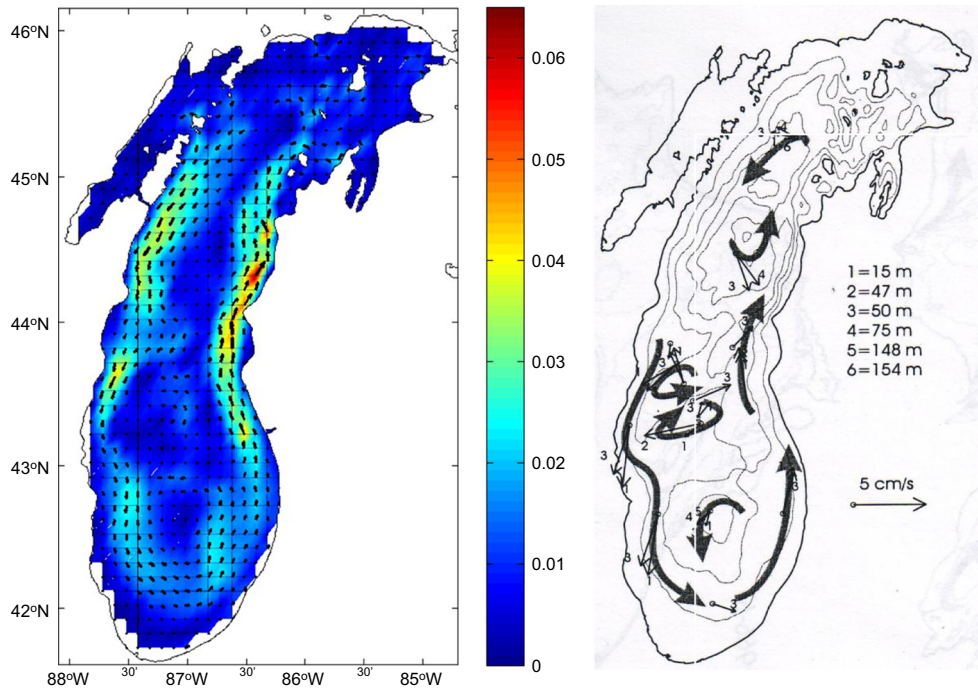

Fig. 4 Modeled (*left*) and observed (*right*, [Beletsky et al., 1999]) annual-averaged current in Lake Michigan

derivation of chl-a data along the coast, in particular near river mouths. Therefore, CDOM should be taken into account in derivation of chl-a in Lake Michigan, which needs in-depth investigations. Since there may still be large uncertainty in the CPA algorithm in Lake Michigan during the twentieth-century's strongest El Niño warming event in 1998, marking a climate shift by Van Cleave et al. (2014), we use NASA data for this study.

The monthly variability of lake-average surface chlorophyll concentration is shown in Fig. 6. The model results with/without river input could capture the observed seasonal change, including the chlorophyll peaks from April to June and October. The comparisons between model results and remote-sensed data indicate that the nutrient source input from tributaries contributed to the growth of phytoplankton in Lake Michigan. However, the model with river input overestimates the lake-wide chl-a from March to July, but matches with the observation from August to December. On the contrary, the model with no river input matches with the observation during March to July, while under-estimates chl-a from August to December (Fig. 6a).

To investigate this in more detail, the lake was divided at 44 N into northern and southern region. It is shown that the model simulates well the chl-a in the northern lake over the seasonal cycle in the river-loading case, while overestimates chl-a in the southern lake, indicating a complex, perhaps different ecosystem in the south than the north because the effect of zebra mussel was not included in the present model. One obvious feature is that the river input raised the entire nutrient level and then the phytoplankton level over the lake. There are several reasons that may be responsible for the discrepancy: (1) the observed satellite data may contain large uncertainty, (2) the model may be too simple to represent both northern and southern lakes, and (3) the forcing data describing the river loaded nutrients may contain large uncertainty.

Table 2 shows the statistics for the comparison. The simulated mean value (1.48 mg/m^3) with river-loaded nutrient matches well with the observed value (1.37 mg/m^3) and

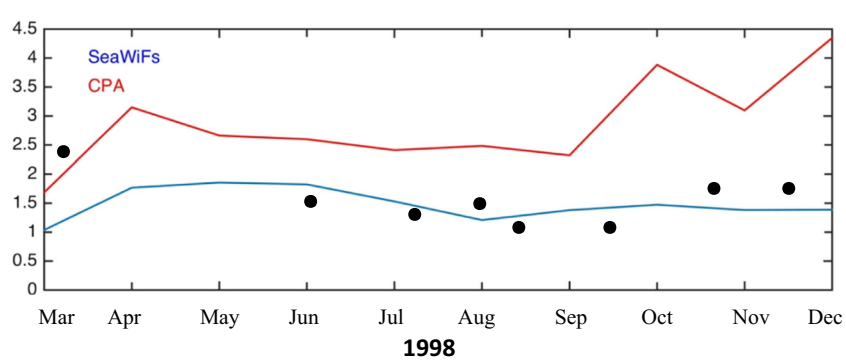

Fig. 5 Lake-wide monthly averaged chl-a time series derived from CPA (Shuchman et al. 2013) and NASA SeaWiFS algorithm. *Dots* are the spatial-averaged surface chl-a from EEGLE transects and towed measurements

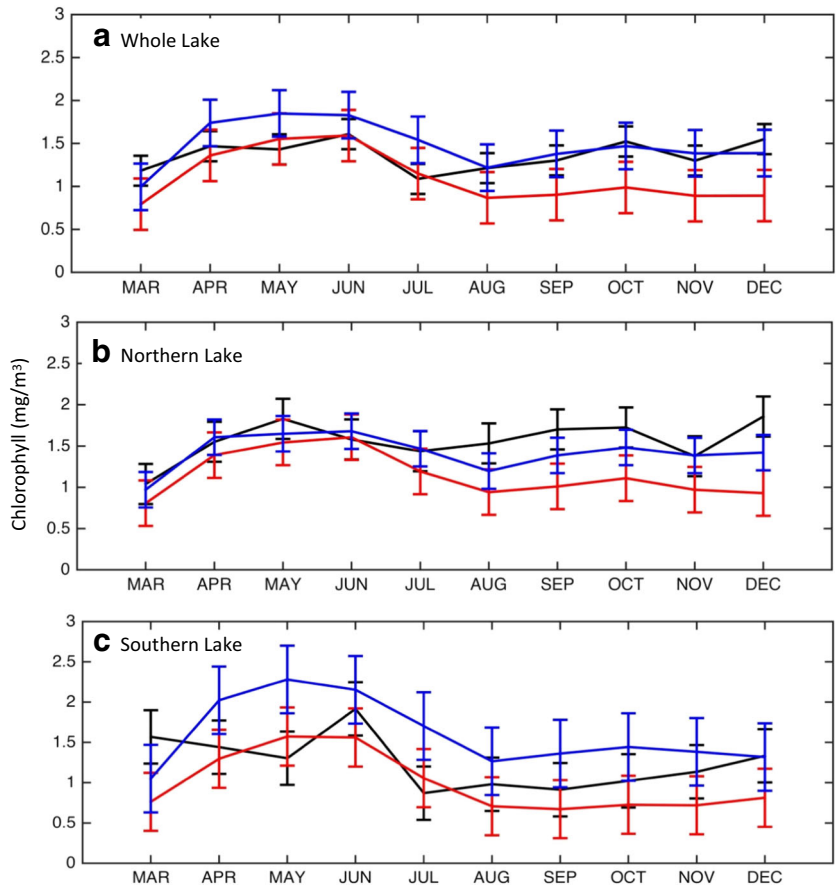

Fig. 6 Temporal (monthly) comparison of the domain-averaged surface chlorophyll concentration (mg m^{-3}) between the SeaWiFS measurement (*black line*) and simulated by FVCOM with (*blue*) and without (*red*) riverine nutrient input from March to December 1998 for whole lake (**a**), northern lake (**b**), and southern lake (**c**). The *vertical bars* are the corresponding temporal standard deviations

exceeds the value (1.1 mg/m^3) without the river-loaded nutrient. Total chlorophyll was underestimated without the nutrient supplement from rivers around the lake. The mean value, STD, MBD, and RMSD indicated the model results were better with nutrient input from rivers than without them. It is shown that the MBD with nutrient input is 8.6% less than half of MBD without nutrient input (−19.6%). The RMSD with nutrient input is 0.24 mg/m^3, much lower than the RMSD (0.37 mg/m^3) without the nutrient input (Table 2).

3.3 Donut-like phytoplankton bloom

Nutrient inputs from tributaries around the lake were added into the model. The new model results showed that, in March, the donut-like phytoplankton bloom had a high chlorophyll concentration along the coast (Fig. 7) and a low chlorophyll concentration in the central portion of southern Lake Michigan. In April, the phytoplankton bloom moved toward the basin center, and the interior diameter of the donut became smaller than that in March. The donut structure of the phytoplankton bloom began to decay in May, while the chlorophyll concentration was still higher in coastal waters than offshore. The modeled patterns of surface chlorophyll concentration matched well with the satellite images. This indicates the importance of riverine nutrient input for maintaining the donut-like phytoplankton bloom in southern Lake Michigan during March to May.

Table 2 Model–data comparison in their mean, STD, MBD, and RMSD with phosphorus (P) and without P

	Mean (mg/m^3)	STD (mg/m^3)	MBD	RMSD (mg/m^3)
SeaWiFS	1.37	0.17		
Model w/o P	1.10	0.30	−19.59%	0.37
Model w. P	1.48	0.27	8.6%	0.24

3.4 The phytoplankton bloom in June 1998

There was a surprising early summer phytoplankton bloom that occurred in southern Lake Michigan as seen from SeaWiFS images. Lesht et al. (2002) determined that the phytoplankton bloom increased rapidly on 2 June (day 153) to a peak level on 22 June (day 173). After the peaking, chl-a decreased rapidly in mid-July. They analyzed the satellite images and in situ measurements and hypothesized that the bloom was triggered by a brief wind event that caused substantial vertical mixing that brought the nutrient-rich deep water into the epilimnion, even though the lake was already stratified.

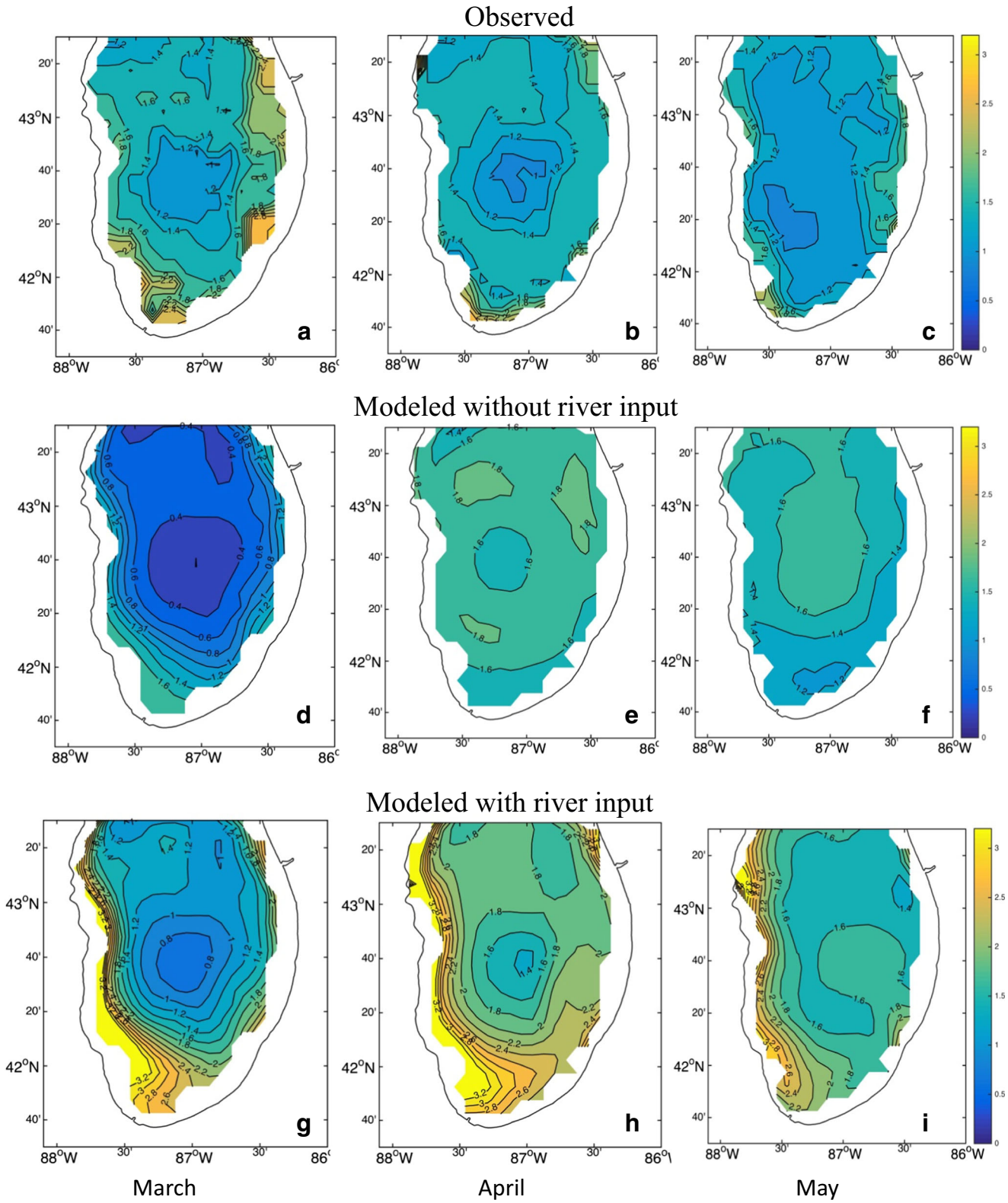

Fig. 7 Monthly averaged SeaWiFS image and simulated surface chlorophyll concentration (mg/m^3) with and without riverine input in March, April, and May 1998

We selected three successive 8-day averaged chlorophyll data from the SeaWiFS images in which the short-term bloom was shown clearly from June 10 to July 3 (Fig. 8). The observed bloom has also contained patches with very high

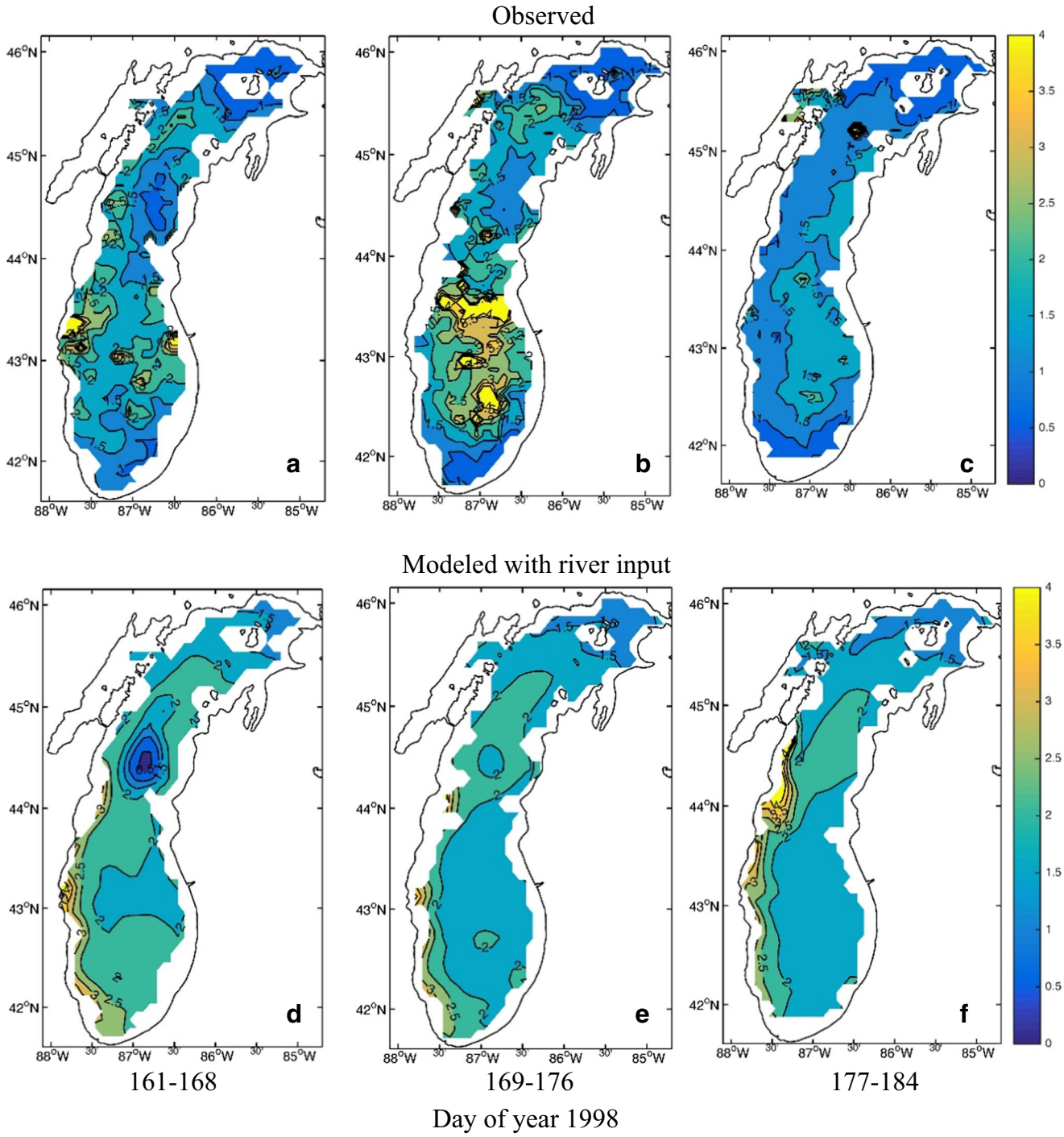

Fig. 8 The 8-day averaged SeaWiFS image and simulated surface chlorophyll concentration (mg/m^3) from June 10 to July 3, 1998

chlorophyll concentration—even higher than 10 mg/m^3 during the peak period (days 169–176). However, the model only reproduced a weak bloom (3 mg/m^3) in central southern Lake Michigan (Fig. 8b vs e). The model results show strong bloom along the west coast throughout the period.

To reveal why the model could not reproduce this strong bloom in terms of physical processes, we examined the time series of 10-m wind speed above the surface, thermal structure, and chlorophyll concentration in a central point of southern Lake Michigan (Fig. 9). The time series covers the entire phytoplankton bloom event. The point location is the same as the one measured by Lesht et al. (2002). The wind speed was derived from the station meteorological data, which were interpolated from the meteorological stations around the lake. It can be seen that an abrupt intense wind event occurred on June 2. After the wind event, the surface temperature

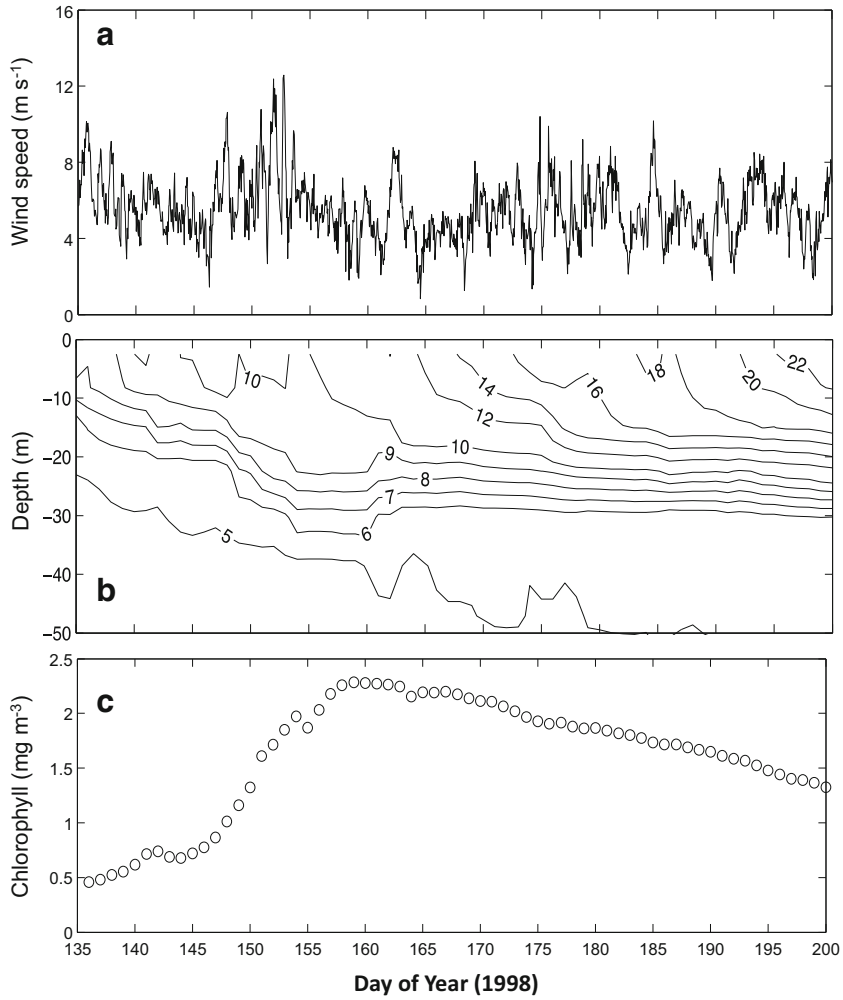

Fig. 9 Time series of (**a**) wind speed at 5 m above the water surface interpolated from the meteorological stations around the lake, (**b**) modeled water temperature profiles, and (**c**) modeled chl-a concentration at buoy CM1 (see Fig. 1, *right*) during the abrupt phytoplankton bloom event. (Units are in m/s for wind speed, °C for temperature, and mg/m^3 for chl-a)

dropped, and the mixed layer deepened to 20 m. The concurrent chlorophyll (chl-a) concentration reached a peak and decreased in the following days. This implies that our model reflected the timing well of the phytoplankton bloom initiated by the brief wind event. However, the magnitude was very week. Therefore, the weak vertical mixing derived from wind-forcing (that deepened the mixed layer to 20 m only) was insufficient to support the strong phytoplankton bloom because the nutrient-rich water could not be pumped up to the surface layer. This also indicates that vertical mixing scheme in physical model may need further improvement in order to accurately simulate the phytoplankton bloom.

Figures 7 and 8 show the discrepancy that the nearshore-offshore gradients in the model are much stronger than in observations in the donut bloom (Fig. 7). In the case of the June bloom, modeled chlorophyll is higher nearshore than offshore while in observations it is higher offshore than nearshore (Fig. 8b vs f). The major reason here is that the ecosystem model lacks of a zebra mussel process that rapidly grew along the coast in the late 1990s, as observed by Nalepa et al. (2014). They showed (see Fig. 8 of Nalepa et al.) high abundance of zebra mussel along the coast of Lake Michigan. This should be a major missing biological process. This same mechanism was identified by Vanderploeg et al. (2007; see their Fig. 13), who observed in situ chl-a values nearshore that were much lower than the N-P-Z model of Chen et al. (2004), because the model did not include the feeding activities (processes) of abundant zebra mussels nearshore.

3.5 High phytoplankton concentration in Green Bay

Green Bay is a shallow bay, with maximum depth of less than 40 m. This allows for faster warming than in Lake Michigan, which in turn, results in faster phytoplankton growth. There are several main rivers around the bay. The Menominee River and Fox River in the southern part of the bay have high flow with peak values of larger than 400 m^3/s. The total phosphorus load is 792 MTA (million tons per year) in the southern part of the bay and 148 MTA in the northern bay. The high nutrient loads keep high primary production high in the southern part of the bay.

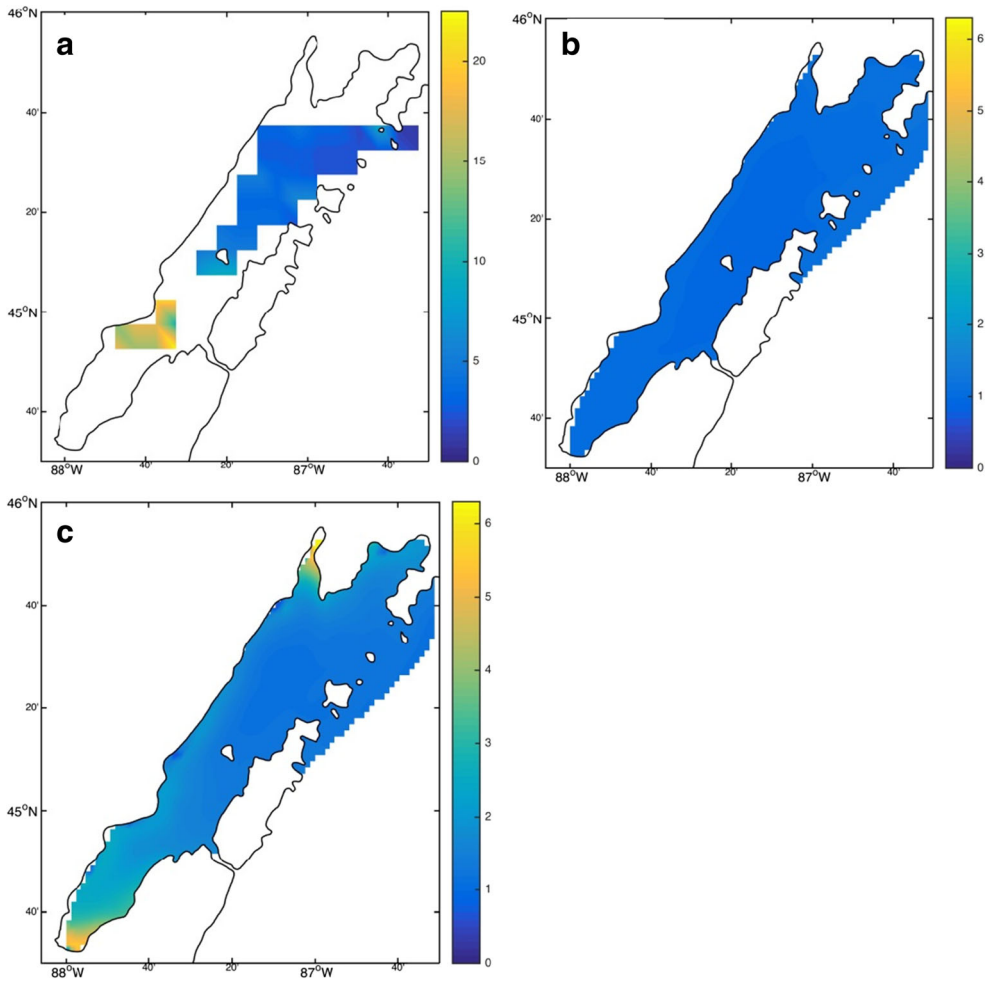

Fig. 10 Annual-averaged SeaWiFS image (**a**) and simulated surface chlorophyll concentration (mg/m^3) without (**b**) and with (**c**) river input in Green Bay

The phytoplankton concentration in Green Bay remained high throughout the year except when the bay was covered by ice. The spring–summer averaged SeaWiFS data were used to validate the model results of chlorophyll concentration in Green Bay with and without riverine nutrients input (Fig. 10). The model shows that a high chlorophyll concentration occurred in Green Bay when the model was forced by the external loading of nutrients. On the contrary, without the riverine loading, the phytoplankton was much lower than the observation.

The simulated bay-wide annual averaged chlorophyll concentration was only 2.8 mg/m^3—more than twice lower than the observation of 6.5 mg/m^3 (Fig. 11). This indicates that the model does not catch the magnitude of the observations. The major possible reason may be that the observations in Green Bay contain high CDOM that should be removed from the calculation of chl-a (Mouw et al. 2013; Shuchman et al. 2013). The other possible reason is that the river loading was underestimated to support the strong bloom. Missing data, as shown in Fig. 10, due to satellite resolution and cloud

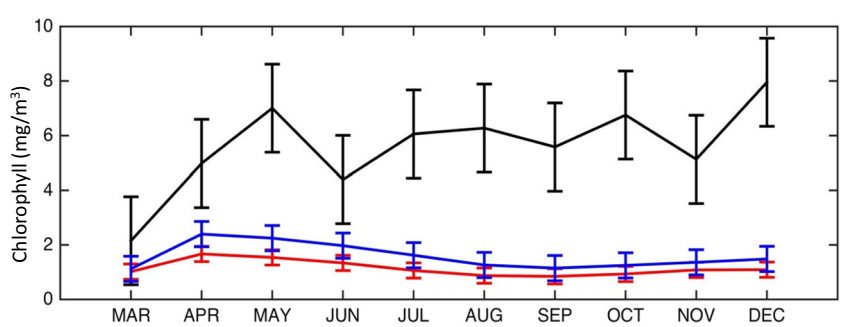

Fig. 11 Same as Fig. 6, except in Green Bay

cover, may also introduce uncertainty to the SeaWiFS data, since the limited number of available high data points might lead to biased high average value. The simulation with river loading, although lower than the observations, is closer to the observation than without river loading (Fig. 11).

4 Concluding remarks

Nutrient loads from 19 rivers (phosphorus) were added to an existing 3-D, coupled physical–biological, 4-compartment NPZD model (Luo et al. 2012). The model was applied to Lake Michigan in 1998. In addition, water currents and vertical and horizontal temperature structure were reasonably well simulated. Results were validated with both satellite and in situ data. In addition, a side-by-side comparison of the effect with and without nutrient loads from rivers on the spring to early summer bloom in Lake Michigan was conducted.

The model can depict the phytoplankton bloom during spring and summer. With the riverine nutrient loads, the donut-like bloom between March and May was reproduced, whereas the bloom existed for 1 month only without nutrient load input. A detailed statistical comparison (Table 2) was conducted to show that a coupled physical–biological model needs external nutrient forcing to sustain a seasonal bloom from spring to early summer and indicates that river runoff and nutrient loads are very important to accurately reproduce lake conditions. Therefore, continuous monitoring and gauging of river runoff and nutrient loading is the key to successful ecosystem forecasting in the Great Lakes.

The model reproduces the monthly bloom (Fig. 7) in southern Lake Michigan from March to May, but overestimated magnitude. On the other hand, the synoptic bloom even in June (Fig. 8) was poorly simulated, with underestimated magnitude. The major reason is that the biological model was highly simplified to the ecological processes in Lake Michigan. For example, zebra mussel processes were not included, while observation showed zebra mussels were a potentially important factor during the late 1990s (Vanderploeg et al. 2007; Nalepa et al. 2014, see their Fig. 8). The physical model did not produce sufficient vertical mixing in response to the strong wind event to bring the nutrient-rich water up to the surface layer to support the strong chl-a bloom in central Lake Michigan. Therefore, an improved vertical mixing scheme is a key to reproducing phytoplankton bloom driven by a strong wind event.

The large magnitude of CPA data compared to the SeaWiFS data indicates that the influence of CDOM on derivation of chl-a is large nearshore and near river mouths such as in Green Bay. An improved algorithm should be developed to remove CDOM from the chl-a concentration in Lake Michigan.

Acknowledgements We appreciate the support from EPA Great Lakes Restoration Initiative to the climate change project awarded to Drs. B. Lofgren and J. Wang. Thanks also go to Nicole Rice for editing the draft. This is GLERL Contribution No. 1865. Luo appreciates support by the National Natural Science Foundation of Guangdong, China (2014A030313777) and from the Overseas Partnership Innovative Project of SCSIO.

Appendix A: The mathematical expressions for each term of Eqs. (1)–(4) are given as

$$P(uptake) = \mu^P_{\max} \cdot \mu(T) \cdot \mu(I) \cdot \mu(N)P \tag{a1}$$

$$P(respiration) = \gamma_P \cdot P\exp\left(\gamma^T \cdot T\right) \tag{a2}$$

$$Z(respiration) = \gamma_Z \cdot Z\exp\left(\gamma^T \cdot T\right) \tag{a3}$$

$$D(remineralization) = d^R \cdot D\exp\left(\gamma^T \cdot T\right) \tag{a4}$$

$$ZP(grazing) = G_{\max}\frac{\sigma_P P}{1+\sigma_P P+\sigma_D D}Z \tag{a5}$$

$$ZD(grazing) = G_{\max}\frac{\sigma_D D}{1+\sigma_P P+\sigma_D D}Z \tag{a6}$$

$$P(mortality) = \varepsilon_P P \tag{a7}$$

$$Z(mortality) = \varepsilon_Z Z \tag{a8}$$

$$P(\sin king) = -w_P\frac{\partial P}{\partial z} \tag{a9}$$

$$D(\sin king) = -w_D\frac{\partial D}{\partial z} \tag{a10}$$

where the definition of each parameter in the equations (a1–a10) is given in Appendix B.

Appendix B

Table 3 Biological model parameters

Parameter	Definition	Value used
$\mu^P_{\max}$	Maximum growth rate for P	2.8 day^{-1}
K_s	Half-saturation constant for the N uptake by P	0.6 mmol P m^{-1}
γ_Z	Zoo respiration coefficient	0.015 day^{-1}
γ_P	Phyto respiration coefficient	0.01 day^{-1}
γ^T	Exponential for Temperature forcing	0.07
d^R	Remineralization rate of detritus	0.015 day^{-1}
$G_{\max}$	Maximum P grazing rate by Z	0.4 day^{-1}
σ_P	Preference coefficient of Z on P	0.5 (mmol C m^{-3})$^{-1}$
σ_D	Preference coefficient of Z on D	0.1 (mmol C m^{-3})$^{-1}$
ε^Z	Assimilation efficiency of Z	0.35
ε_P	Mortality rate of P	0.01 day^{-1}

Table 3 (continued)

Parameter	Definition	Value used
ε_Z	Mortality rate of Z	0.02 day $^{-1}$
$\lambda_{Chl:C}$	Ratio of chlorophyll to carbon (C)	0.34 mg Chl/mmol C
w_P	Sinking velocity of P	0.6 m day $^{-1}$
w_D	Sinking velocity of D	0.6 m day $^{-1}$

References

Bai X, Wang J, Schwab DJ, Yang Y, Luo L, Leshkevich GA, Liu S (2013) Modeling 1993–2008 climatology of seasonal general circulation and thermal structure in the Great Lakes using FVCOM. Ocean Model 65:40–63

Beletsky D, Saylor JH, Schwab DJ (1999) Mean circulation in the Great Lakes. J Great Lakes Res 25(1):78–93. https://doi.org/10.1016/S0380-1330(99)70718-5

Beletsky D, Schwab DJ (2001) Modeling circulation and thermal structure in Lake Michigan: annual cycle and interannual variability. J Geophys Res 106(C9):19,745–19,771

Beletsky D, Schwab DJ, Roebber PJ, McCormick MJ, Miller GS, Saylor JH (2003) Modeling wind-driven circulation during the March 1998 sediment resuspension event in Lake Michigan. J Geophys Res 108(C2):3038. https://doi.org/10.1029/2001JC001159

Beletsky D, Schwab D, McCormick M (2006) Modeling the 1998–2003 summer circulation and thermal structure in Lake Michigan. J Geophys Res 111:C10010. https://doi.org/10.1029/2005JC003222

Beletsky D, Schwab D (2008) Climatological circulation in Lake Michigan. Geophys Res Lett 35:L21604. https://doi.org/10.1029/2008GL035773

Bennington V, McKinley GA, Kimura N, Wu CH (2010) General circulation of Lake Superior: mean, variability, and trends from 1979 to 2006. J Geophys Res 115:C12015. https://doi.org/10.1029/2010JC006261

Bennington V, McKinley GA, Urban NR, McDonald CP (2012) Can spatial heterogeneity explain the perceived imbalance in Lake Superior's carbon budget? A model study. J Geophys Res 117: G03020. https://doi.org/10.1029/2011JG001895

Chapra SC, Sonzogni WC (1979) Great Lakes total phosphorus budget for the mid 1970s. J Water Pollut Control Fed:2524–2533

Chen C, Ji R, Schwab DJ, Beletsky D, Fahnenstiel GL, Jiang M, Johengen TH, Vanderploeg H, Eadie B, Budd JW, Bundy MH, Gardner W, Cotner J, Lavrentyev PJ (2002) A model study of the coupled biological and physical dynamics in Lake Michigan. Ecol Model 152:145–168

Chen C, Wang L, Ji R, Budd JW, Schwab DJ (2004) Impacts of suspended sediment on the ecosystem in Lake Michigan: a comparison between the 1998 and 1999 plume events. J Geophys Res 109: C10S05. https://doi.org/10.1029/2002JC001687

Chen C, Beardsley RC, Cowles G (2006) An unstructured-grid, finite-volume Coastal Ocean Model (FVCOM) system. Oceanography 19(1):78–89. https://doi.org/10.5670/oceanog.2006.92

Hu H, Wang J (2010) Modeling effects of tidal and wave mixing on circulation and thermohaline structures in the Bering Sea: process studies. J Geophys Res 115:C01006. https://doi.org/10.1029/2008JC005175

Ji R, Chen C, Budd JW, Schwab DJ, Beletsky D, Fahnenstiel GL, Johengen TH, Vanderploeg HA, Eadie BJ, Cotner J, Gardner W, Bundy M (2002) Influences of suspended sediments on the ecosystem in Lake Michigan: a 3-D coupled bio-physical modeling experiment. Ecol Model 152:169–190

Kerfoot WC, Budd JW, Green SA, Cotner JB, Biddanda BA, Schwab DJ, Vanderploeg HA (2008) Doughnut in the desert: late-winter production pulse in southern Lake Michigan. Limno Oceanography 53(2): 589–604

Lesht BM, Fontaine TD III, Dolan DM (1991) Great Lakes total phosphorus model: post audit and regionalized sensitivity analysis. J Great Lakes Res 17(1):3–17

Lesht BM, Stroud JR, McCormick MJ, Fahnenstiel GL, Stein ML, Welty LJ, Leshkevich GA (2002) An event-driven phytoplankton bloom in southern Lake Michigan observed by satellite. Geophys Res Lett 29(8):1177. https://doi.org/10.1029/2001GL013533

Li, R., C. Chen, H. Xia, R. C. Beardsley, M. Shi, Z. Lai, H. Lin, Y. Feng, C. Liu, Q. Xu, Y. Ding, Y. Zhang (2014). Observed wintertime tidal and subtidal currents over the continental shelf in the northern South China Sea. J Geophys Res, 22. Doi:10.1002/2014JC009931

Luo L, Wang J, Schwab DJ, Vanderploeg H, Leshkevich G, Bai X, Hu H, Wang D (2012) Simulating the 1998 spring bloom in Lake Michigan using a coupled physical-biological model. J Geophys Res 117: C10011. https://doi.org/10.1029/2012JC008216

Nalepa, T.F., D.L. Fanslow, G.A. Lang, K. Mabrey, and M. Rowe, 2014. Lake-wide benthic surveys in lake michigan in 1994-95, 2000, 2005, and 2010: abundances of the amphipod *diporeia spp.* and abundances and biomass of the mussels *dreissena polymorpha* and *dreissena rostriformis bugensis*. NOAA Technical Memorandum GLERL-164, 25pp

Mouw CB, Chen H, McKinley GA, Effler S, O'Donnell D, Perkins MG, Strait C (2013) Evaluation and optimization of bio-optical inversion algorithms for remote sensing of Lake Superior's optical properties. J Geophys Res Oceans 118:1696–1714. https://doi.org/10.1002/jgrc.20139

Oveisy A., R.R. Yerubandi, L.F. Leon, and S.A. Bocaniov (2014). 3-D winter modeling and effects of ice cover on hydrodynamics. Thermal structure and water quality in Lake Erie. J Great Lakes Research (in press)

Powers CF, Ayers JC (1960) Water transport studies in the straits of Mackinac region of Lake Huron. Limnol Oceanogr 5:81–85

Pilcher DJ, McKinley GA, Bootsma HA, Bennington V (2015) Physical and biogeochemical mechanisms of internal carbon cycling in Lake Michigan. J Geophys Res Oceans 120:2112–2128. https://doi.org/10.1002/2014JC010594

Rowe, M., E. Anderson, J. Wang, and H. Vanderploeg, 2015. Modeling the effect of invasive quagga mussels on the spring phytoplankton bloom in Lake Michigan. J Great Lakes Res. 41:17 pp. https://doi.org/10.1016/j.jglr.2014.12.018113

Saylor JH, Sloss PW (1976) Water volume transport and oscillatory current flow through the Straits of Mackinac. J Phys Oceanogr 6:229–237. https://doi.org/10.1175/1520-0485(1976)006<0229:WVTAOC>2.0.CO;2

Shuchman RA, Leshkevich G, Sayers MJ, Johengen TH, Brooks CN, Pozdnyakov D (2013) An algorithm to retrieve chlorophyll, dissolved organic carbon, and suspended minerals from Great Lakes satellite data. J. Great Lakes Res. Suppl 39:14–33

Tian R, Chen C, Qi J, Ji R, Beardsley RC, Davis C (2014) Model study of nutrient and phytoplankton dynamics in the Gulf of Maine: patterns and drivers for seasonal and interannual variability. ICES J Mar Sci. https://doi.org/10.1093/icesjms/fsu090

Vanderploeg HA et al (2007) Anatomy of the recurrent coastal sediment plume in Lake Michigan and its impacts on light climate, nutrients, and plankton. J Geophys Res 112:C03S90. https://doi.org/10.1029/2004JC002379

Van Cleave K, Lenters JD, Wang J, Verhamme EM (2014) A regime shift in Lake Superior ice cover, evaporation, and water temperature

following the warm El Niño winter of 1997-98. Limnol Oceanogr 59(6):1889–1898. https://doi.org/10.4319/lo.2014.59.6.1889

Wang D-R, Yang Y, Wang J, Bai X (2015) A modeling study of the effects of river runoff, tides, and surface wind-wave mixing on the eastern and western Hainan upwelling systems of the South China Sea. China *Ocean Dyn*. https://doi.org/10.1007/s10236-015-0857-3

Wang J (1996) Global linear stability of the two-dimensional shallow water equations: application of the distributive theorem of roots for polynomials on the unit circle. Mon Wea Rev 124(6):1301–1310. https://doi.org/10.1175/1520-0493(1996)124<1301:GLSOTT>2.0.CO;2

Wang J, Hu H, Schwab D, Leshkevich G, Beletsky D, Hawley N, Clites A (2010) Development of the Great Lakes Ice-circulation model (GLIM): application to Lake Erie in 2003-2004. J Great Lakes Res 36:425–436. https://doi.org/10.1016/j.jglr.2010.04.002

White B, Austin J, Matsumoto K (2012) A three dimensional model of Lake Superior with ice and biogeochemistry. J Great Lakes Res 30(1):61–71